

Computational study of the electronic and geometric structures of the dihalogenodimethylselenium compounds, Me_2SeX_2 ($\text{X} = \text{F}, \text{Cl}, \text{Br}, \text{I}$ or At)[†]

Nikolas Kaltsoyannis*

Centre for Theoretical and Computational Chemistry, University College London,
20 Gordon Street, London, UK WC1H 0AJ

The dihalogenodimethylselenium compounds Me_2SeX_2 ($\text{X} = \text{F}, \text{Cl}, \text{Br}, \text{I}$ or At) have been studied computationally using quasi-relativistic density functional theory. For Me_2SeX_2 ($\text{X} = \text{F}, \text{Cl}$ or Br), the most stable structure is calculated to be the hyperco-ordinate C_{2v} symmetric ψ -trigonal-bipyramidal geometry. By contrast, the charge-transfer C_s -symmetric 'spoke' structures, which obey the octet rule, are found to be the most stable form of Me_2SeI_2 and Me_2SeAt_2 . This change in structural type with increasing halogen atomic number is in agreement with previous X-ray crystallographic studies. The factors that determine the most stable structure are found to be intramolecular in origin. The preference for the ψ -trigonal-bipyramidal geometry of Me_2SeX_2 ($\text{X} = \text{F}, \text{Cl}$ or Br) is traced to the much greater bond-strength difference between Se-X and X-X for the lighter halogens. Analysis of the intramolecular charge distributions and molecular orbital compositions indicated that the Se-X bond polarity decreases significantly with increasing halogen atomic number. This is in agreement with previous theoretical studies, which indicate that hyperco-ordinate systems are favoured by highly polar bonds to the central atom. No evidence was found for significant involvement of the selenium d orbitals in the Se-X or Se-C bonding in hyperco-ordinate Me_2SeX_2 .

The geometric structures of the products of the reaction of diorganoselenium compounds with dihalogens continues to be a subject of considerable interest. For example, the diphenyl derivatives Ph_2SeX_2 ($\text{X} = \text{Cl}^{\dagger}$ or Br^{\ddagger}) both adopt the ψ -trigonal-bipyramidal structure.[‡] X-Ray crystallography was recently employed to show that this geometry is also favoured by Me_2SeCl_2 and Me_2SeBr_2 , but that the charge-transfer molecular 'spoke' structure ($\text{Me}_2\text{Se-I-I}$) is adopted by the diiodine compound.³ This change in structural type is also found in some of the closely related triorgano Group 15 compounds, R_3EX_2 ($\text{R} = \text{Me}, \text{Ph}$ or Me_3C). Thus while R_3AsI_2 and Me_3AsBr_2 all adopt the charge-transfer geometry, Ph_3AsBr_2 is trigonal bipyramidal.⁵

Which of these two structures is adopted depends upon a number of factors. It has been suggested that, if the E atom in R_3EX_2 ($\text{E} = \text{Group 15 element}$) is more acidic than the halogen, then the trigonal-bipyramidal structure is favoured.⁵ Conversely, the charge-transfer 'spoke' structure is adopted if X is more acidic than E. The acidity of E is affected by the R group to which it is attached. Electron-donating R groups increase the basicity of E and thus favour the charge-transfer geometry. The solvent from which the compounds are crystallised is also found to play a major role, in that polar solvents favour the charge-transfer adduct (stabilising what, in the limit, may be regarded as $\text{R}_3\text{EX}^+\text{X}^-$). These arguments are equally applicable to R_2SeX_2 .

The ψ -trigonal-bipyramidal geometry is, of course, the result of the Se atom being surrounded by five electron pairs. It is therefore hyperco-ordinate, and Cooper *et al.*⁴ have pointed out that the stability of such molecules of p-block elements beyond the second period is closely related to the polarity of the bonds to that element. Given the range of electronegativities of the halogens,⁶ this argument is clearly worthy of consideration in the present investigation.

This contribution reports the results of a computational study of Me_2SeX_2 ($\text{X} = \text{F}, \text{Cl}, \text{Br}, \text{I}$ or At ; ψ -trigonal-bipyramidal and charge-transfer structures), using quasi-relativistic^{7,8} density functional theory.⁹ The aims of this work were to see if the theoretical approach employed could reproduce correctly the structural change from ψ -trigonal bipyramidal to charge-transfer at $\text{X} = \text{I}$ and, if so, to provide an explanation as to why the change occurs. Clearly this investigation takes no account of solvent effects as each molecule is studied in isolation, but it is of interest to determine if the structural change is driven by intra- rather than inter-molecular effects. Although no experimental data exist for Me_2SeF_2 and Me_2SeAt_2 , they were included in the present study to allow comparison within the entire family of Me_2SeX_2 , and to establish if there is a trend in the favoured structure as Group 17 is descended.

The accuracy with which density functional methods can calculate molecular properties such as ground and transition-state geometries, bond-dissociation energies, electronic transition and ionisation energies is in many cases at least as good as that of high-level *ab initio* techniques.¹⁰⁻¹² This is particularly so for compounds containing one or more heavy elements (*e.g.* d- and f-block atoms) which are often intractable by sophisticated *ab initio* calculations (*i.e.* those involving significant electron-correlation procedures). The computational requirements of density functional calculations is a key factor, typically scaling as N^3 in the number of electrons as compared with N^5 to N^7 for Hartree-Fock + correlation approaches. Thus density functional methods in general yield accurate, reliable information on heavy-element compounds at a fraction of the computational cost of high-level *ab initio* calculations, and are particularly attractive when applied, as in the present study, to a series of molecules in which one or more atoms are varied from light ($\text{F}, Z = 9$) to very heavy ($\text{At}, Z = 85$).

Computational Details

All calculations were performed with the Amsterdam Density Functional program suite.^{13,14} Quasi-relativistic frozen cores were used for all elements bar H; C (1s), F (1s), Cl (2p), Se (3d),

* E-Mail: n.kaltsoyannis@ucl.ac.uk.

[†] Supplementary data available (No. SUP 57308, 11 pp.): vibrational wavenumbers. See *J. Chem. Soc., Dalton Trans.*, 1997, Issue 1.

Non SI unit employed: eV $\approx 1.60 \times 10^{-19}$ J.

[‡] This nomenclature is quite common (see, for example, ref. 3 and refs. therein) although the term disphenoidal⁴ is also in widespread use.

Table 1 Calculated and experimental (in italics) bond lengths (Å) and angles (°) for the ψ -trigonal-bipyramidal (ψ -tbp) and charge-transfer (ct) structures of Me_2SeX_2 (X = F, Cl, Br, I or At). Atom labels in column 1 refer to Fig. 1

	Me_2SeF_2	$\text{Me}_2\text{SeCl}_2^a$	$\text{Me}_2\text{SeBr}_2^a$	$\text{Me}_2\text{SeI}_2^a$	Me_2SeAt_2
ψ -tbp					
Se–X	1.923	2.411, 2.379 ^b	2.579, 2.549 ^b	2.810	2.866
Se–C ^c	1.953	1.968	1.971	1.977	1.977
C–H	1.100 ^b	1.100 ^b	1.101 ^b	1.101 ^b	1.100 ^b
X–Se–X	172.0	178.1, 177.8	179.8, 177.7	178.6	178.3
X–Se–C	87.4	89.4, 91.7 ^b	90.0, 90.8 ^b	90.5	90.6
C–Se–C	96.9	96.0, 98.6	95.9, 98	95.7	95.4
Se–C–H	106.2 ^b	106.1 ^b	106.2 ^b	106.3 ^b	106.2 ^b
ct					
Se–X ¹	2.031	2.553	2.693	2.932, 2.916	3.014
X ¹ –X ²	1.775	2.225	2.502	2.846, 2.768	2.956
Se–C ^c	1.954	1.963	1.966	1.967	1.967
C–H	1.101 ^b	1.100 ^b	1.101 ^b	1.101 ^b	1.100 ^b
X ² –X ¹ –Se	171.3	174.0	174.5	174.0, 174.3	175.2
X ¹ –Se–C	89.8	91.7	93.4	92.8, 96.2	93.7
C–Se–C	95.1	95.0	95.1	94.9, 99	95.3
Se–C–H	107.4 ^b	107.7 ^b	107.8 ^b	107.9 ^b	107.9 ^b
X–X in ct/X–X in freeX ₂ ^d	1.24	1.12	1.10	1.07	

^a Experimental data from ref. 3. ^b Average. ^c Experimental Se–C bond lengths not given in ref. 3. ^d Experimental data from ref. 19.

Br (3d), I (4d) and At (5d). Relativistic core potentials were computed using the ADF auxiliary program DIRAC. An uncontracted double-zeta Slater-type orbital valence basis set was employed for all atoms, supplemented with a single p polarisation function for H and a d function for all other atoms (ADF Type III). For I and At no polarisation function is provided by default, and hence d functions with exponents of 2.2 and 2.4 respectively were added to the ADF Type II double-zeta valence basis sets. The molecular geometries were fully optimised at the local level using the density functional of Vosko, Wilk and Nusair (VWN),¹⁵ and were confirmed as true energy minima by the observation of only positive eigenvalues in the Hessian matrix and hence no imaginary vibrational wavenumbers. The calculated vibrational wavenumbers of all ten target molecules are available as SUP 57308. The molecular and fragment bonding energies were then computed at the optimised geometries using the VWN functional in conjunction with Becke's gradient correction¹⁶ to the exchange part of the potential and the correlation correction due to Lee, *et al.*¹⁷ (ADF 'postscf' option). Mulliken population analyses were performed.¹⁸

The calculations were performed on an IBM RS/6000 43P-166 workstation and the EPSRC's six-processor DEC 8400 'Columbus' superscalar computer.

Results and Discussion

Optimised geometries

Ball-and-stick representations of the ψ -trigonal-bipyramidal (C_{2v} symmetry) and charge-transfer 'spoke' (C_s) structures of Me_2SeX_2 are given in Fig. 1(a) and (b) respectively. Table 1 contains the calculated bond lengths and angles for all ten Me_2SeX_2 molecules studied, together with the X-ray crystallographic data for Me_2SeCl_2 , Me_2SeBr_2 and Me_2SeI_2 .³ Comparison of the theoretical and experimental structural data reveals a close match. The Se–X bond lengths are slightly overestimated by the calculations, although the greatest discrepancy is only 0.032 Å for Se–Cl in ψ -trigonal-bipyramidal Me_2SeCl_2 . Somewhat poorer agreement is found for the only X–X bond for which an experimental value is available, with a 0.078 Å difference between the calculated and experimental I–I distance in charge-transfer Me_2SeI_2 . The agreement between the calcu-

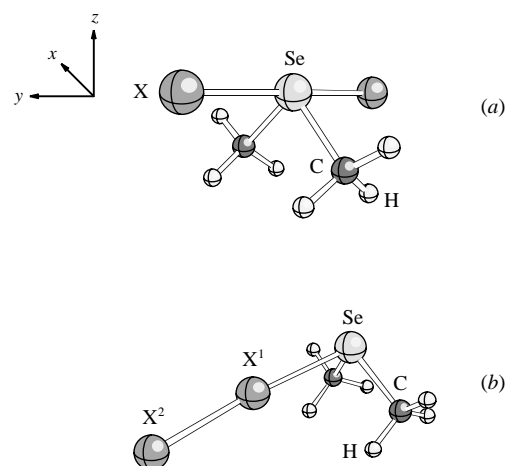


Fig. 1 Ball-and-stick representations of the (a) ψ -trigonal-bipyramidal and (b) charge-transfer structures of Me_2SeX_2 (X = halide)

lated and experimental bond angles is very good ($<4^\circ$) in all cases. Hence the calculations reproduce the experimental geometries extremely well, lending credence to the other theoretical data discussed below.

Electronic structure

Fig. 2 is a molecular orbital (MO) energy-level diagram for all five C_{2v} symmetric ψ -trigonal-bipyramidal Me_2SeX_2 . As might be expected, the valence electronic structures of these molecules are quite similar to one another, with the energies of the MOs with significant halogen content differing most from molecule to molecule. A group theoretical analysis reveals that the Se–C σ bonds transform as $a_1 + b_1$ in the axis system shown on Fig. 1(a), the Se–X σ bonds span $a_1 + b_2$ and the halogen p_π orbitals transform as $a_1 + a_2 + b_1 + b_2$. In addition to these MOs, it might be expected that there will be another MO of a_1 symmetry in the valence region, corresponding to the formal selenium lone-pair. It is, of course, possible that mixing of orbital character will occur in MOs of the same symmetry, and that some of the valence levels may have a C–H bonding component.

Rather than discuss the MO structure of each of the five C_{2v}

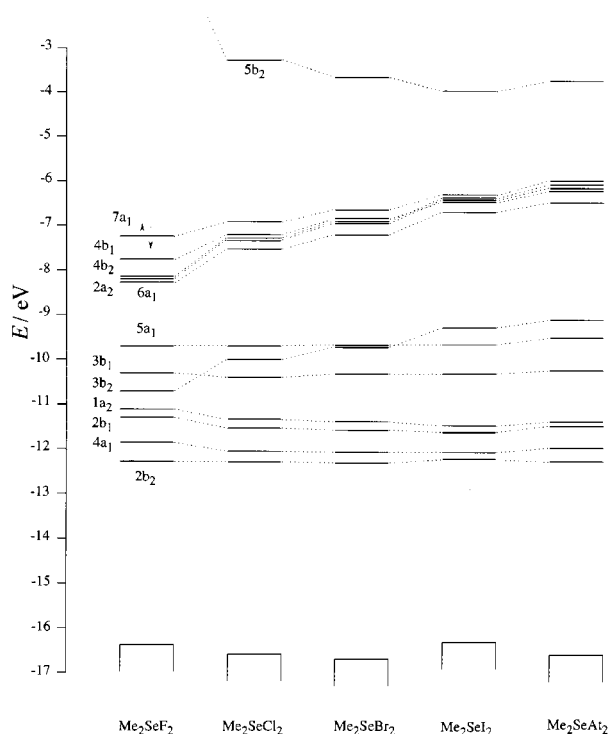


Fig. 2 Molecular orbital energy-level diagram for ψ -trigonal-bipyramidal Me_2SeX_2 ($\text{X} = \text{halogen}$), C_{2v} symmetry. The highest occupied orbital is the $7a_1$.

Me_2SeX_2 in turn, I shall take Me_2SeCl_2 as a representative example. The MOs $2a_2$ to $4b_1$ are chlorine p_π -based lone-pair orbitals, as illustrated by the contour plot of the $4b_2$ MO shown in Fig. 3(a). The $3b_2$ MO [Fig. 3(b)] is Se–Cl σ bonding, with a smaller C–H σ component. By contrast, the $2b_2$ is mainly C–H σ bonding, with some Se–Cl σ . The $3b_1$ level is both Se–C and C–H σ bonding, as is the $2b_1$ MO. The $1a_2$ MO is exclusively C–H bonding. The greatest mixing of orbital character occurs in the valence levels of a_1 symmetry. The $4a_1$ is mainly C–H bonding, although there is a smaller Se–C σ component. The $6a_1$ and $7a_1$ are predominantly chlorine p_π -localised, although there is some Se–Cl antibonding character in the $6a_1$ level [Fig. 3(c)]. If any of the a_1 symmetry MOs can be identified as the selenium lone-pair orbital it is the $5a_1$ [Fig. 3(d)], although there is also substantial Se–C and C–H σ bonding in this level. Finally we have the $5b_2$ lowest unoccupied MO (LUMO), which is very strongly Se–Cl σ antibonding [Fig. 3(e)].

It is clear from Fig. 2 that MOs $6a_1$ to $7a_1$ and the $3b_2$ orbital are significantly stabilised as the atomic number of the halogen becomes smaller, while the other orbitals are largely unaffected. Those MOs whose energies do change are those with large halogen p character, and the changes are entirely as expected on electronegativity grounds.

Fig. 4 presents valence MO energy-level schemes for all five C_s -symmetric charge-transfer Me_2SeX_2 . There are many similarities between these schemes and Fig. 2, not the least of which is that both diagrams have 12 occupied MOs in the energy range -5 to -13 eV. The halogen p_π lone-pair orbitals are the $6a'' + 11a'$ and $5a'' + 9a'$ levels, the energies of which clearly follow the electronegativity of the halogen atoms. The selenium 'lone pair' MO is the $8a'$ level, although as with the ψ -trigonal-bipyramidal molecules this orbital is not exclusively Se based. A contour plot of the $8a'$ MO of Me_2SeCl_2 is shown in Fig. 5(a), from which it may be seen that this orbital is also Se–Cl and Cl–Cl bonding. The bonding of the Se to the X_2 unit is a classic three-level system, as illustrated by the contour plots of the $7a'$ [Fig. 5(b)], $10a'$ [Fig. 5(c)] and $12a'$ [Fig. 5(d)] MOs of charge-transfer Me_2SeCl_2 . The $7a'$ MO is bonding between the Se–Cl and Cl–Cl. The $10a'$ level is mainly localised on the Se and the Cl furthest from the Se, and is largely Se–Cl and Cl–Cl non-

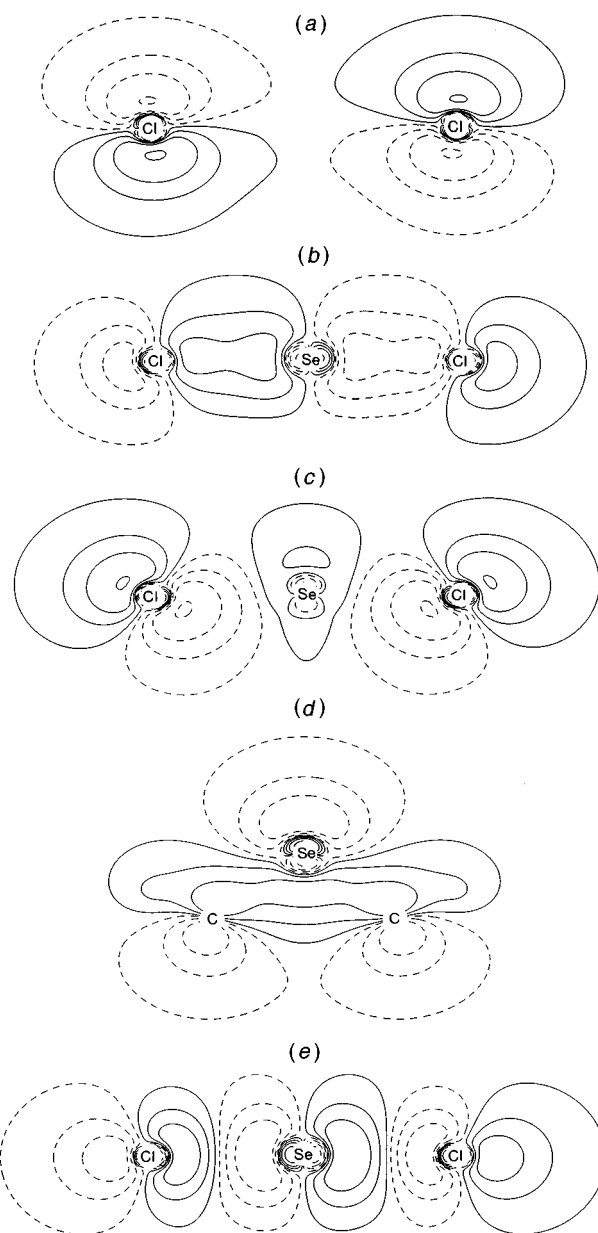


Fig. 3 Contour plots of the (a) $4b_2$, (b) $3b_2$, (c) $6a_1$, (d) $5a_1$ and (e) $5b_2$ molecular orbitals of ψ -trigonal-bipyramidal Me_2SeX_2 ($\text{X} = \text{halide}$). Contour levels are ± 0.2 , ± 0.1 , ± 0.05 and ± 0.03 . All plots are in the yz plane [see Fig. 1(a) for axis system] except that of $5a_1$ which is in the xz plane

bonding. By contrast, the $12a'$ LUMO is very strongly antibonding along the Se–Cl–Cl unit.

In recent years a large body of theoretical evidence has built up to suggest that the ability of p-block atoms in the third period and below to 'expand their octet' (*i.e.* to have more than four electron pairs around them) has very little to do with the involvement in the bonding of d orbitals on the central atom (*via*, for example, hybridisation schemes such as d^2sp^3 , dsp^2 and dsp^3).^{4,20–22} Indeed, Cooper *et al.*⁴ have suggested that the octet rule be replaced by what they term the 'democracy principle'; any valence electron can participate in chemical bonding given sufficient energetic incentive. The role of d orbitals in these compounds is at most as polarisation functions. The present study is entirely in agreement with this argument, in that none of the valence MOs in any of the five hyperco-ordinate ψ -trigonal-bipyramidal molecules has significant selenium d character (the *greatest* selenium d content is a 3.52% contribution to the $6a_1$ MO of Me_2SeF_2). This almost negligible d-orbital participation is no greater than in the charge-transfer molecules, which formally obey the octet

Table 2 Calculated bonding energies (kJ mol^{-1}) of the ψ -trigonal-bipyramidal and charge-transfer structures of Me_2SeX_2 (X = F, Cl, Br, I or At)

Structure	Fragment			$\text{Me}_2\text{Se/X}_2$	$\text{Me}_2\text{Se/X} + \text{X}$	Total	Conclusion
	Me_2Se	X_2	$\text{X} + \text{X}$				
Me_2SeF_2 (ψ -tbp)	-4197		+15		-807	-4989	ψ -tbp more stable by 289 kJ mol^{-1}
Me_2SeF_2 (ct)	-4200	-241		-259		-4700	
Me_2SeCl_2 (ψ -tbp)	-4200		+40		-482	-4642	ψ -tbp more stable by 74 kJ mol^{-1}
Me_2SeCl_2 (ct)	-4203	-279		-86		-4568	
Me_2SeBr_2 (ψ -tbp)	-4200		+40		-384	-4544	ψ -tbp more stable by 33 kJ mol^{-1}
Me_2SeBr_2 (ct)	-4203	-233		-75		-4511	
Me_2SeI_2 (ψ -tbp)	-4202		+35		-284	-4451	ct more stable by 11 kJ mol^{-1}
Me_2SeI_2 (ct)	-4204	-206		-52		-4462	
Me_2SeAt_2 (ψ -tbp)	-4200		+35		-271	-4436	ct more stable by 23 kJ mol^{-1}
Me_2SeAt_2 (ct)	-4204	-207		-48		-4459	

rule. Thus the present calculations provide further evidence that it is not necessary to invoke d-orbital participation in order to explain the bonding in hyperco-ordinate molecules. The valence MO structures of ψ -trigonal-bipyramidal Me_2SeX_2 may be understood perfectly adequately with only s and p functions on the Se atom.

Bonding energies

Table 2 contains calculated bonding-energy data for all ten target molecules. The total molecular bonding energy (the energy of the molecule *versus* its atomic fragments at infinite separation) is in each case broken down into smaller components; Me_2Se and $\text{X} + \text{X}$ for the ψ -trigonal-bipyramidal structures and Me_2Se and X_2 for the charge-transfer geometry. In all cases the fragments are calculated at their positions in the optimised geometries for the whole molecule.

It is gratifying that the present calculations predict that the change from ψ -trigonal-bipyramidal structures to charge-transfer geometry should occur between Br and I, in agreement with the X-ray crystallographic data.^{3,§} There is a clear trend, with the lighter halogens favouring the ψ -trigonal-bipyramidal structure and the charge-transfer geometry gaining in relative stability as Group 17 is descended. As might be expected (and confirmed by the data in the second column of Table 2), this change has very little to do with the Me_2Se fragment. The bonding energy within this fragment is essentially the same in all cases.

Although there are differences in the bonding energy of the X_2 and $\text{X} + \text{X}$ fragments as the halogen is altered, these are small when compared with the changes in the $\text{Me}_2\text{Se/X}_2$ and $\text{Me}_2\text{Se/X} + \text{X}$ data. For Me_2SeF_2 , the bonding energy of Me_2Se with the two F atoms in the ψ -trigonal-bipyramidal structure is so much greater (548 kJ mol^{-1}) than that between the Me_2Se and F_2 fragments in the charge-transfer molecule that the additional contribution due to the F_2 fragment falls well short of tipping the overall balance in favour of the charge-transfer molecule. As the halogen becomes heavier, however, the bonding-energy difference between $\text{Me}_2\text{Se/X}_2$ and $\text{Me}_2\text{Se/X} + \text{X}$ becomes much smaller (only 232 kJ mol^{-1} for X = I), with the result that the bonding within the X_2 fragment acquires

§ It should be noted that the molecular geometries were optimised at the local level, and gradient corrections were then applied at these geometries to determine the bonding energies (as described in Computational Details). Additional calculations were also performed on ψ -trigonal-bipyramidal and charge-transfer Me_2SeBr_2 and Me_2SeI_2 , in which the gradient corrections were included self-consistently (an approach which is far more demanding in terms of computing time). Although the optimised geometries were in poorer agreement with experiment than those obtained at the local level, the relative molecular stabilities were almost exactly the same as those given in the last column of Table 2, *i.e.* a change in structural type is predicted between Me_2SeBr_2 and Me_2SeI_2 by both computational approaches.

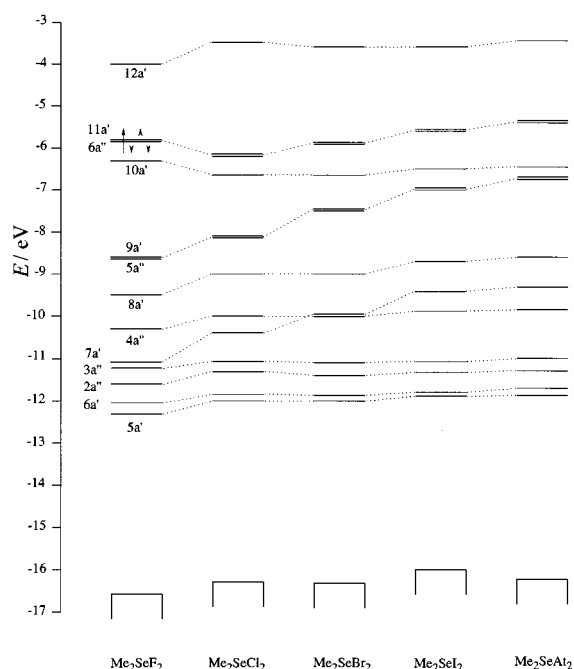


Fig. 4 Molecular orbital energy-level diagram for charge-transfer Me_2SeX_2 (X = halogen), C_s symmetry. The highest occupied orbital is the $11a'$

greater significance. The change in structural type between the lighter halogens and the I and At molecules may therefore be traced to the relative strengths of two Se-X bonds *versus* one Se-X and one X-X. For the lighter halogens, the former are much more favoured, but the weaker Se-X bonding of the heavier halogens brings the bonding energy of the X_2 unit more into play.

In their work on hyperco-ordinate third-period atoms, Cooper *et al.*⁴ concluded that 'the feasibility of hyperco-ordinate systems seems to be dependent on the possibility of making significantly polar bonds which shift electron density away from the central atom'. This argument elegantly rationalises, for example, the fact that SF_4 adopts the hyperco-ordinate ψ -trigonal-bipyramidal geometry whereas SCl_4 is best formulated as $\text{SCl}_3^+\text{Cl}^-$. We may examine how the present study relates to the assertion of Cooper *et al.* by considering the calculated charges on the atoms within the ψ -trigonal-bipyramidal molecules, which are collected in Table 3. The difference between the charges of two atoms is clearly a measure of the polarity of the bond between them. As might be expected, the charge on the Se atom decreases as the halogen becomes heavier (and less electronegative). Although the charge on the halogens also decreases in the same order, the difference between the charge on the Se and that on the halogens bonded to it is much

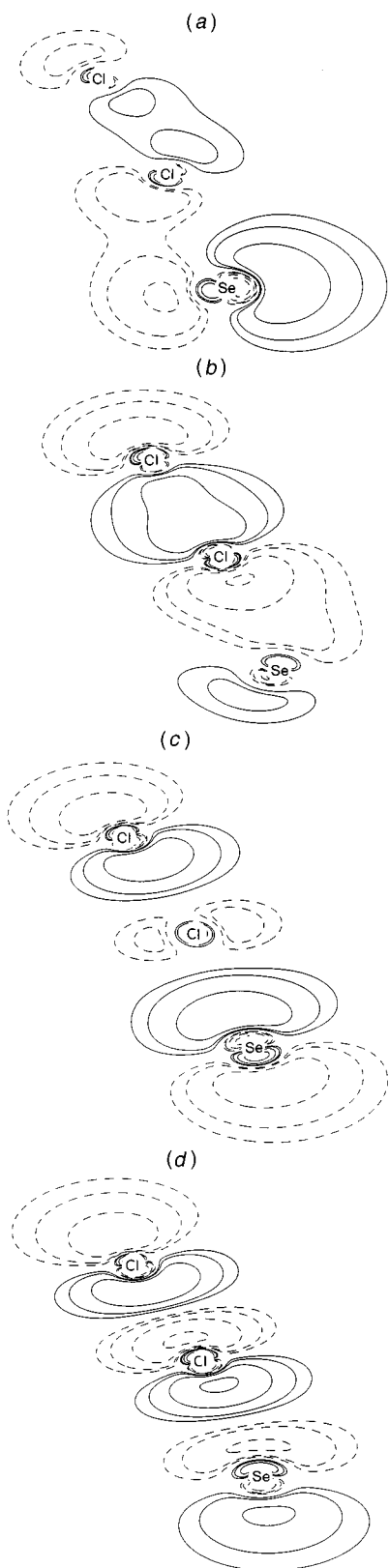


Fig. 5 Contour plots of the (a) $8a'$, (b) $7a'$, (c) $10a'$ and (d) $12a'$ molecular orbitals of ψ -trigonal-bipyramidal Me_2SeX_2 ($X = \text{halide}$). Contour levels are ± 0.2 , ± 0.1 , ± 0.05 and ± 0.03 . All plots are in the molecular mirror plane

greater for $X = \text{F}$ than for $X = \text{I}$ and At . Thus we may conclude that the polarity of the Se-X bond is greatest in Me_2SeF_2 and decreases as Group 17 is descended, a variation which is entirely consistent with the relative electronegativities of the halogens.

We might expect that alterations in Se-X bond polarity with changes in the halogen atom would manifest themselves in the

Table 3 Atomic charges within ψ -trigonal-bipyramidal Me_2SeX_2 ($X = \text{F, Cl, Br, I}$ or At)

Compound	Charge		
	Se	X	$\Delta(\text{Se} - \text{X})$
Me_2SeF_2	+0.953	-0.537	+1.490
Me_2SeCl_2	+0.592	-0.407	+0.999
Me_2SeBr_2	+0.468	-0.343	+0.811
Me_2SeI_2	+0.256	-0.222	+0.478
Me_2SeAt_2	+0.092	-0.112	+0.204

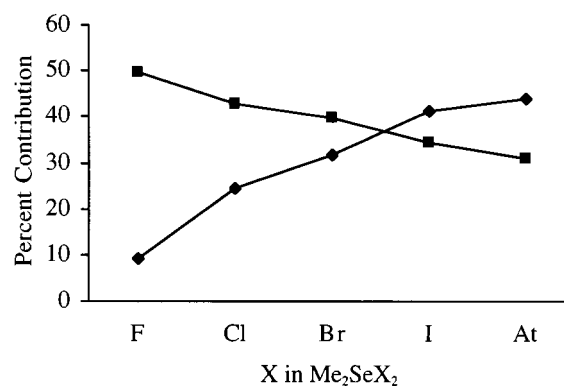


Fig. 6 Percent contribution of the selenium p (diamonds) and halogen p (squares) atomic orbitals to the $3b_2$ molecular orbital of ψ -trigonal-bipyramidal Me_2SeX_2 ($X = \text{halide}$)

composition of MOs with significant Se-X bonding character, for example the Se-X $3b_2$ bonding MO. Fig. 6 plots the contribution of the selenium p and halogen p atomic orbitals to this level of all five ψ -trigonal-bipyramidal Me_2SeX_2 . Although the situation is slightly confused by appreciable contributions from C and H, it is clear that the selenium character of this orbital increases significantly with increasing halogen atomic number, and that the halogen content decreases. As the halogen becomes lighter, the Se-X component of this MO becomes increasingly localised on the halogen atom, supporting the conclusions drawn from the atomic charge differences. It would therefore appear that the assertion of Cooper *et al.* is supported by the present study, in that the most polar Se-X bond is found to be that in Me_2SeF_2 , which is also calculated to be by far the most stable hyperco-ordinate molecule.

The calculated charges on the atoms within the charge-transfer molecules are collected in Table 4. We may use these data to gain some indication of how accurate the term 'charge transfer' is in describing the structure in Fig. 1(b). The charge on the X_2 unit, as given in the column labelled $\text{X}^1 + \text{X}^2$, is clearly greatest for $X = \text{F}$ and least for $X = \text{At}$, although in all cases there is a build-up of charge on the X_2 group. As has been noted before,³ the transfer of electron density from Me_2Se to X_2 should result in a lengthening of the X-X bond, as the electron density enters an X-X σ^* MO. We may test this hypothesis by comparing the total charge on X_2 with the X-X bond length in charge-transfer Me_2SeX_2 and that in free X_2 . The relevant data are given in the last row of Table 1, from which it may be seen that the greatest X-X lengthening is indeed in Me_2SeF_2 , in agreement with the $\text{Me}_2\text{Se} \rightarrow \text{X}_2$ charge-transfer being greatest in this molecule.

Conclusion

The present computational study reproduces the experimentally observed change in structural type in Me_2SeX_2 ($X = \text{F, Cl, Br, I}$ or At) from hyperco-ordinate ψ -trigonal-bipyramidal to charge-transfer at $X = \text{I}$ and, as no account is taken of solvent effects, suggests that it has an intramolecular origin (at least in part). The preference for the ψ -trigonal-bipyramidal geometry

Table 4 Atomic charges within charge-transfer Me₂SeX₂ (X = F, Cl, Br, I or At). Atom labels refer to Fig. 1(b)

Compound	Charge					
	Se	X ¹	X ²	X ¹ + X ²	Δ (Se - X ¹)	Δ (X ¹ - X ²)
Me ₂ SeF ₂	+0.552	-0.301	-0.374	-0.675	+0.853	+0.073
Me ₂ SeCl ₂	+0.307	-0.156	-0.247	-0.403	+0.463	+0.091
Me ₂ SeBr ₂	+0.256	-0.102	-0.247	-0.349	+0.358	+0.145
Me ₂ SeI ₂	+0.205	-0.052	-0.195	-0.247	+0.257	+0.143
Me ₂ SeAt ₂	+0.101	+0.020	-0.167	-0.147	+0.081	+0.187

of Me₂SeX₂ (X = F, Cl or Br) is traced to the much greater bond-strength difference between Se-X and X-X for the lighter halogens. Previous studies have suggested that hyperco-ordinate molecules are favoured by highly polar bonds to the central atom, and that conclusion is reinforced by the present investigation. Analysis of the intramolecular charge distributions and molecular orbital compositions reveals that the Se-X bond polarity decreases significantly with increasing halogen atomic number, as anticipated on electronegativity grounds. The contribution of the selenium d functions to the valence molecular orbitals of all ten target compounds is found to be insignificant. This further strengthens previous theoretical conclusions that the ability of p-block atoms in the third period and below to 'expand their octet' has very little to do with the involvement in the bonding of d orbitals on the central atom.

Acknowledgements

I am grateful to the Royal Society for an equipment grant, and the EPSRC for a grant of CPU time on the 'Columbus' central computing facility. I also wish to thank the referees for their helpful comments.

References

- 1 J. D. McCullough and G. Hamburger, *J. Am. Chem. Soc.*, 1942, **64**, 508.
- 2 J. D. McCullough and G. Hamburger, *J. Am. Chem. Soc.*, 1941, **63**, 303.
- 3 S. M. Godfrey, C. A. McAuliffe, R. G. Pritchard and S. Sarwar, *J. Chem. Soc., Dalton Trans.*, 1997, 1031.
- 4 D. L. Cooper, T. P. Cunningham, J. Gerratt, P. B. Karadakov and M. Raimondi, *J. Am. Chem. Soc.*, 1994, **116**, 4414.
- 5 N. Bricklebank, S. M. Godfrey, H. P. Lane, C. A. McAuliffe, R. G. Pritchard and J. M. Moreno, *J. Chem. Soc., Dalton Trans.*, 1995, 3873.
- 6 J. E. Huheey, E. A. Keiter and R. L. Keiter, *Inorganic Chemistry*, HarperCollins, New York, 4th edn., 1993.
- 7 T. Ziegler, V. Tschinke, E. J. Baerends, J. G. Snijders and W. Ravenek, *J. Phys. Chem.*, 1989, **93**, 3050.
- 8 N. Kaltsoyannis, *J. Chem. Soc., Dalton Trans.*, 1997, 1.
- 9 R. G. Parr and W. Yang, *Density-Functional Theory of Atoms and Molecules*, Oxford University Press, Oxford, 1989.
- 10 *Top. Curr. Chem.*, 1996, **180-183**.
- 11 *Density Functional Methods in Chemistry*, eds J. K. Labanowski and J. W. Andzelm, Springer, New York, 1991.
- 12 T. Ziegler, *Chem. Rev.*, 1991, **91**, 651.
- 13 G. te Velde and E. J. Baerends, *J. Comput. Phys.*, 1992, **99**, 84.
- 14 ADF(2.3), Department of Theoretical Chemistry, Vrije Universiteit, Amsterdam, 1997.
- 15 S. H. Vosko, L. Wilk and M. Nusair, *Can. J. Phys.*, 1980, **58**, 1200.
- 16 A. Becke, *Phys. Rev. A*, 1988, **38**, 3098.
- 17 C. Lee, W. Yang and R. G. Parr, *Phys. Rev. B*, 1988, **37**, 785.
- 18 R. S. Mulliken, *J. Chem. Phys.*, 1955, **23**, 1833.
- 19 N. N. Greenwood and A. Earnshaw, *Chemistry of the Elements*, Pergamon, Oxford, 1984.
- 20 E. Magnusson, *J. Am. Chem. Soc.*, 1990, **112**, 7940.
- 21 T. P. Cunningham, D. L. Cooper, J. Gerratt, P. B. Karadakov and M. Raimondi, *Int. J. Quantum Chem.*, 1996, **60**, 393.
- 22 T. P. Cunningham, D. L. Cooper, J. Gerratt, P. B. Karadakov and M. Raimondi, *J. Chem. Soc., Faraday Trans.*, 1997, 2247.

Received 8th September 1997; Paper 7/06523J